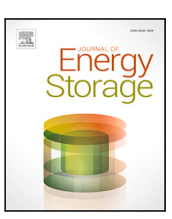
FISEVIER

Contents lists available at ScienceDirect

Journal of Energy Storage

journal homepage: www.elsevier.com/locate/est



Research papers

Electrical safety evaluation of electrolyte leakage of vanadium flow batteries



- ^a School of Chemical Engineering, University of New South Wales, Sydney, NSW, 2052, Australia
- b School of Electrical Engineering & Telecommunications , University of New South Wales, Sydney, NSW, 2052, Australia

ARTICLE INFO

Keywords: Electrical safety Vanadium flow batteries Continuous electrolyte leakage Safety margins

ABSTRACT

Leakage of electrolyte of vanadium flow batteries can cause safety risks due to stray voltage forming on the ground or the surfaces of artificial structures. In this paper, an electrical safety assessment approach is developed using a full electrical equivalent circuit model of multi-stack vanadium flow batteries including the cell voltages and ionic resistance of the electrolyte in the flow channels, manifolds and the pipes between stacks and tanks. This approach applies Gauss's flux law to study the electric field distribution on dielectric surfaces during continuous electrolyte leakage and assesses the risk levels according to the IEC electrical safety standard TS60479. Electrical safety case studies are carried out on scenarios with different battery footing concrete slab dimensions, moisture levels, feet positions, and electrical insulation levels, with safety zones determined.

1. Introduction

In the 1980s, Professor Maria Skyllas-Kazacos at the University of New South Wales and her research team invented the all-vanadium redox flow battery [1–4]. Over the 40 years, vanadium batteries have undergone substantial iterations, leading to remarkable enhancements in the performance of their individual components. Notably, the aqueous-based nature of these batteries renders them inherently safer and more reliable than their conventional lithium-ion counterparts. Compared to other types of redox flow batteries, vanadium batteries leverage the unique advantage of vanadium's four distinct valence states, effectively circumventing cross-contamination of the membrane. As vanadium flow batteries are increasingly integrated into a broader array of infrastructural applications, their safety assessment has become important.

Electrolyte leakage constitutes a significant safety hazard during the operation of flow batteries. Once it occurs, it not only inflicts chemical damage upon those who come into contact with it but also poses a risk of electric shock. During the operation of flow batteries, the electrolyte functions as a charged entity with a specific electric potential. In the event of a persistent leakage, it can generate an electric field over a certain area on the surface of the medium with which it ultimately comes into contact, similar to the electric field formed on the ground when a power transmission line breaks, falls vertically, and establishes contact with the ground. If an individual traverses this area, the distance between their feet can result in a potential difference if both feet are not positioned on an equal-potential surface. This scenario can lead to the formation of a step voltage between the feet, culminating in electric shock.

Whitehead et al. were the first to investigate the risks caused by internal or external short circuits of a single stack vanadium flow battery (VFB). Experimental results showed that both external and internal short-circuits posed no significant safety risks, with the stack maintaining normal operation even under increased hydraulic mass transfer rates [5]. Routh et al. provided an overview of chemical hazards, protective testing, and the risk of electric shock through existing IEC and IEEE standards (e.g., IEC62485, IEEE1578, IEC60364, etc. [6]), including potential scenarios of electrolyte leakage leading to electric shock. Trovò et al. [7] studied potential safety issues associated with flow batteries, mentioning the general risk of electrocution due to leakage. However, there is no quantitative analysis performed on the risks posed by electrolyte leakage.

This paper develops an approach to the analysis of the electric shock risks associated with vanadium flow batteries during ongoing leakage incidents. Equivalent circuit models for the battery systems, the grounding system, and the human body are developed to analyse the maximum current going through the human body. Furthermore, the Finite Element Method (FEM) is used to obtain the electric field distribution and further determine the hazard level according to the electrical safety standard IEC TS60479.

Case studies are conducted to assess the safety risks associated with electrolyte leakage in a VFB system in different scenarios, including the battery system's electrical configuration, the presence or absence of a concrete slab (their dryness and size), the position of human legs, and the type of footwear protection.

E-mail address: m.kazacos@unsw.edu.au (M. Skyllas-Kazacos).

^{*} Corresponding author.

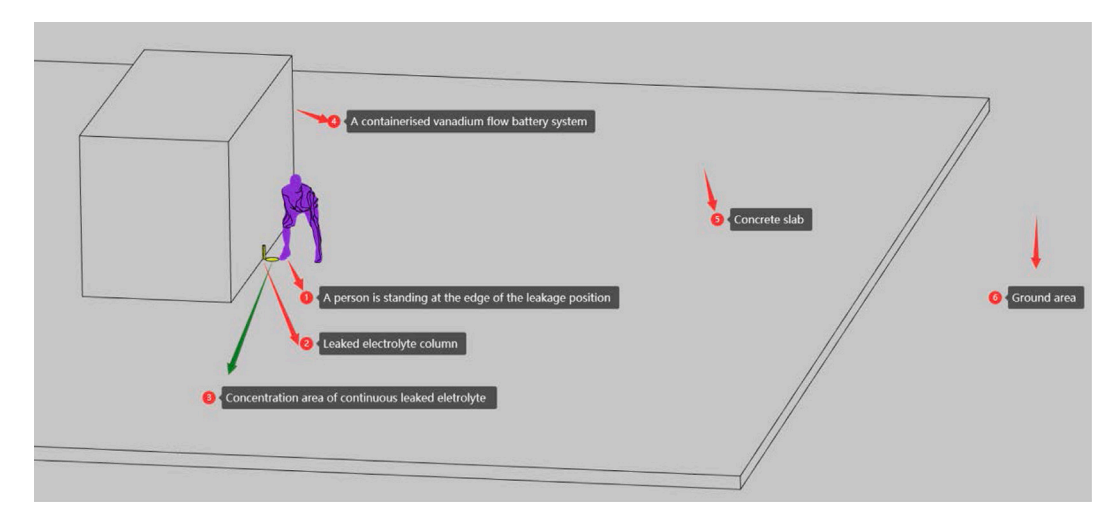


Fig. 1. Electrical shock overview during electrolyte leakage of a containerised VFB system.

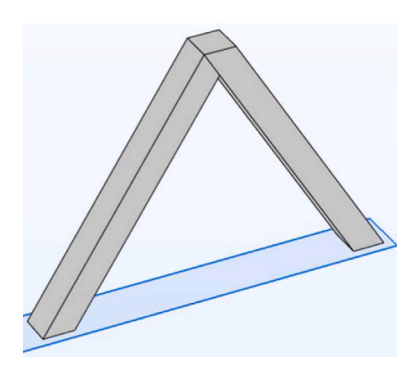


Fig. 2. Human leg-crotch model.

The structure of the paper is organised as follows. The proposed electrical safety analysis method is presented in Section 2, including a problem formulation, the developments of an equivalent circuit model, a grounding system model, a human resistance model, the mechanism of electric field distribution calculation, and an electrical safety assessment procedure. Case studies are presented in Section 3 with a discussion of the results. The paper is concluded in Section 4 with a summary of key findings.

2. Electrical safety analysis for a multi-stack VFB system during continuous electrolyte leakage

This paper develops an electrical safety assessment method to investigate whether continuous electrolyte leakage poses an electric shock risk to individuals near the leakage site of a VFB system. For this assessment, it is essential to calculate the equivalent current flowing through the foot-to-foot path in the human body (denoted as I_{ff} in this paper) when a person's feet are in contact with a surface where the electrolyte has leaked (see Fig. 1). This analysis requires the equivalent circuit models of the VFB during leakage, the grounding system, and the human body. The leaked potential derived through the equivalent circuit model is the voltage formed at the contact surface of the grounding medium surface due to the grounding path created during the continuous electrolyte leakage. Linking to the equivalent circuit model, human leg-crotch model (see Fig. 2), and grounding system model, this potential is part of the potential boundary condition for the analysis of the grounding system to obtain potential and electric field distribution and is a key variable for the electrical safety assessment.

Firstly, the equivalent circuit model of the VFB under electrolyte leakage conditions is proposed in Section 2.1 to obtain the potential

at the accumulated area of electrolyte leakage, denoted as V_1 . To adequately analyse the impact of shunt current on V_1 , the equivalent circuit model includes the ionic resistance of the electrolyte in all VFB piping system.

Secondly, the grounding system's potential and electric field distribution can be attained by using Finite Element Modelling (FEM) analysis as in Section 2.2. The results encompass the potential values at all positions within the grounding system. The human circuit model describes the equivalent resistance along the foot-to-foot current pathway in the electric shock scenario. The difference between maximum and minimum potentials at the feet area of the human model can be obtained through potential distribution, which represents the voltage across the leg-crotch (denoted as V_{pd}). Finally, the current through the human body via foot–foot pathway I_{ff} can be obtained and then convert to the equivalent body current via hand-to-feet pathway I_b , as described in Section 2.3.

2.1. Equivalent electrical circuit model of a multi-stack VFB during electrolyte leakage

2.1.1. Electrical and hydraulic configurations of a VFB system

In the VFB system, the electrolyte is circulated from the tank to the stack via a pump and recirculates back to the tank, forming a continuous hydraulic pathway. In multi-stack configurations, the piping system serves as possible ion transfer pathways, introducing ionic resistance and resulting in parasitic power and energy losses due to shunt currents. Studies have been conducted on the impedance networks of flow battery systems, incorporating more ionic resistances to examine the effects of shunt current [8-22]. However, the ionic resistance of the electrolyte pathways related to the tank has not been considered. The model proposed in this paper is the first to incorporate the ionic resistance of the electrolyte across all fluid pathways within a VFB system, including the ionic resistance of electrolyte in the pipelines between the tank and the stacks, and the pipelines between stacks, the manifolds, and the channels. This model combined with the leakage grounding path provides a comprehensive analysis of system behaviour during leakage in an industrial-scale multi-stack VFB system and offers a reliable model for risk assessments across various application scenarios.

Two electrical topologies are considered during a continuous electrolyte leakage event in this work.

Configuration 1: 2 × n stacks are divided into n groups, each group
has two stacks with electrical series connection and groups of
stacks are electrically connected in parallel shown in Fig. 3(a).

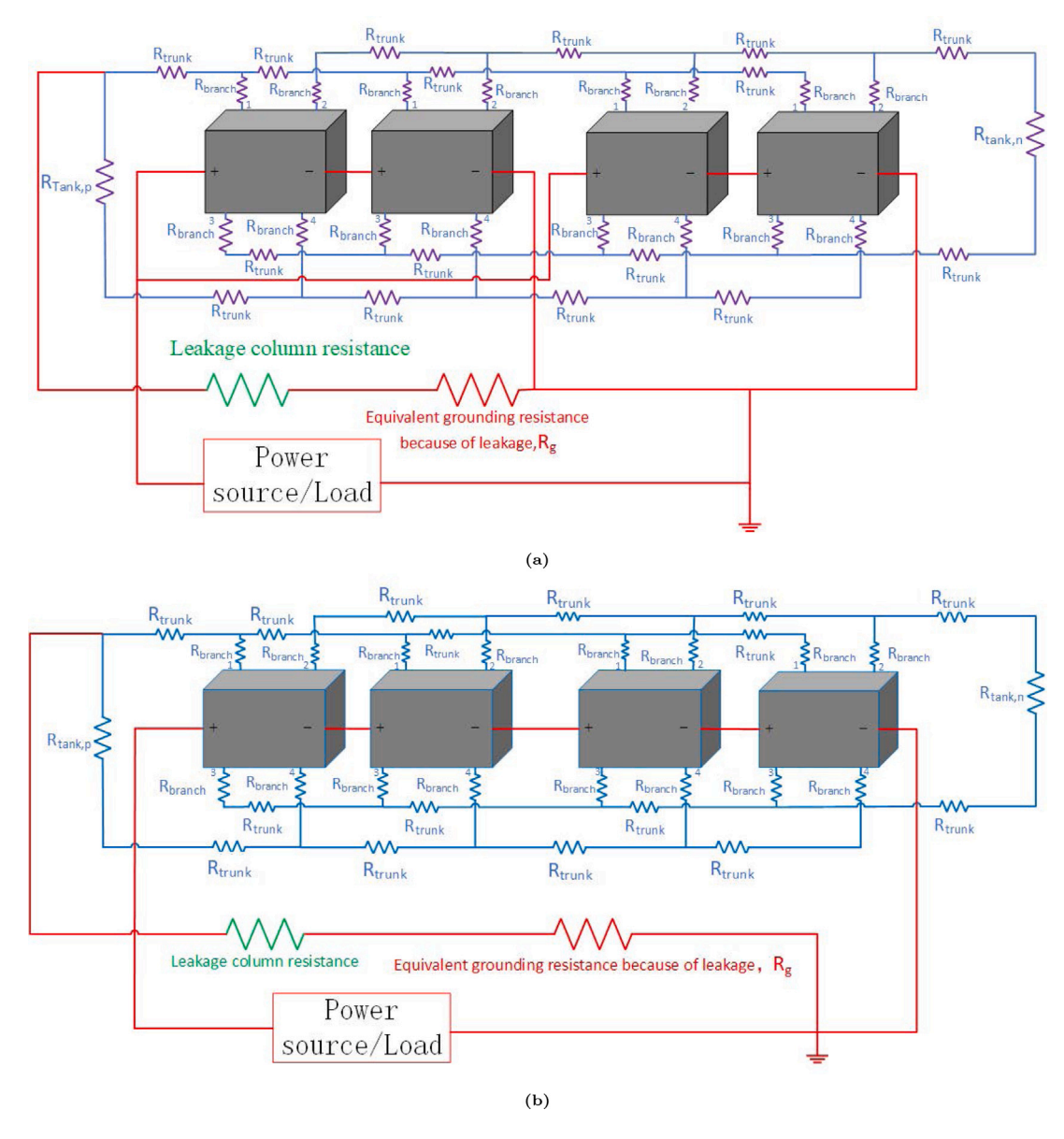


Fig. 3. Electrical circuits of four-stack VFB systems (with peripheral piping, load/power source and a grounding loop formed by the electrolyte leakage at the tank including the equivalent resistance of the grounding system, highlighted in red) for two configurations: (1) 2 stacks connected in series with 2 parallel branches (2P2S) (2) 4 stacks connected in series (1P4S).

 Configuration 2: All stacks are electrically connected in series as described in Fig. 3(b).

Fig. 3(a) presents the VFB system under Configuration 1 during leakage. Fig. 4 illustrates the detail of the equivalent circuit inside grey blocks (stacks) of Fig. 3(a), where V represents the cell voltage, R denotes the cell resistance, m indicates the manifold, c stands for the channel, + refers to the positive half-cell, and - refers to the negative half-cell. $R_{\rm trunk}$ denotes the ionic resistance within the transverse external piping, while $R_{\rm branch}$ represents that within the longitudinal piping. Fig. 3(b) illustrates the electrical connections of a VFB system under Configuration 2 with the same equivalent stack circuit shown in Fig. 4.

2.1.2. Conductivity of the ionic resistance of the VFB system

Shunt current is significantly affected by the ionic resistance of the electrolyte within the pathways. These ionic resistances serve as parasitic elements, thereby diverting a portion of the current supplied by the charger and reducing the overall efficiency of the battery, as illustrated in Fig. 4. In the equivalent circuit, the grounding path acts as an integral component, and current flowing through it is influenced by the resistances in other parts of the circuit. Once the resistance of the grounding path is determined, the current flowing through this path dictates the value of V_1 . The c vanadium ion concentrations of the electrolyte in the positive and negative tanks can be used to calculate the ionic conductivity of the electrolyte in the positive and negative tanks, σ_+ and σ_- respectively, in millisiemens/centimetre, can be calculated from the concentration of the electrolyte [23]:

$$\sigma_{+} = 235 + 46.43 \times C_5^t, \ \sigma_{-} = 160 + 30.5 \times C_2^t$$
 (1)

where C_2^t and C_5^t are concentrations of V^{2+} and V^{5+} (mol/L) in the electrolyte, respectively.

2.2. Mechanism of electric field distribution calculation

The equivalent circuit model during leakage allows for the calculation of the leaked potential V_1 by incorporating the grounding system resistance, denoted as R_g . The value of R_g represents the resistance

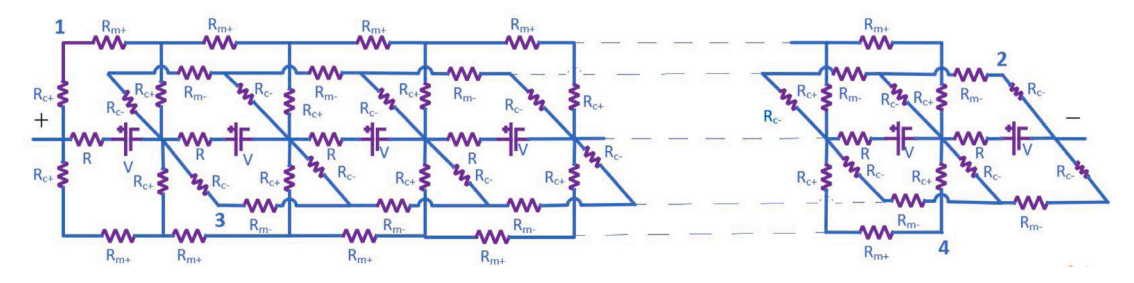


Fig. 4. Electrical circuit in each stack (grey blocks in Fig. 3).

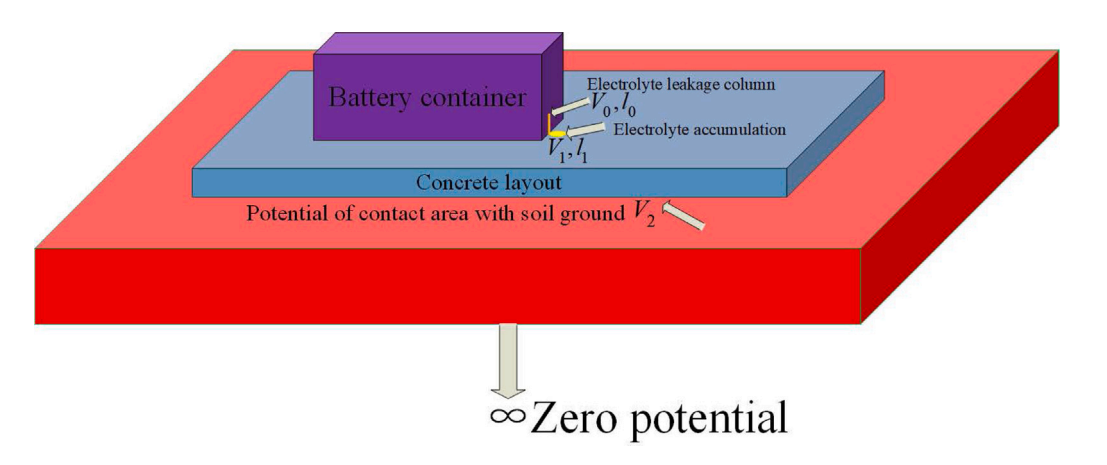


Fig. 5. An equivalent schematic of an electrolyte leakage event in a multi-media interface system.

of the whole grounding system and it varies depending on the composition and characteristics of the grounding system. However, due to the potential and dimensional boundary conditions of the grounding system, the electric field and potential distribution cannot be obtained through simple calculations. FEM analysis can deal with the boundary conditions and provide accurate numerical solutions.

In the FEM analysis, the grounding system model is needed to define the system structure, set material properties, and establish potential boundary conditions. The system is then meshed, and a solver is used to obtain numerical solutions and plot the potential and electric field distributions.

2.2.1. Equivalent grounding resistance and leaked potential analysis

Fig. 5 illustrates an equivalent schematic of an electrolyte leakage occurring in a multi-media interface system, where the VFB system has a potential of V_0 at the leak point with a height of l_0 . The electrolyte falls vertically along the container wall and accumulates on the ground into a circular area with a potential of V_1 and a height of l_1 , which forms an equipotential surface.

An equivalent grounding system consists of three media with respective electrical conductivities: leg-crotch parts (media A) $\sigma_{\rm Leg}$, a concrete slab (media B) $\sigma_{\rm Concrete}$, and soil ground (media C) $\sigma_{\rm Soil}$.

The resistance of the grounding system is invariant as it can be seen as a linear resistor network from the circular area where V_1 locates to the infinitely distant ground. Then the equivalent resistant can be calculated using Thevenin's theorem. V_1 is applied to a circular region on the surface of the concrete slab, and the infinitely distant ground is set to a reference potential ($V_{\rm ground}=0$), which are potential boundary conditions.

FEM will use some first principles to calculate the equivalent resistant. According to Gauss's law [24], the rate of change of charge density Q, the electric field \mathbf{E}_i and the resulting current density \mathbf{J}_i within each medium follow the laws:

$$\nabla \cdot \mathbf{J}_i = Q, \ \mathbf{E}_i = -\nabla V_i \text{ and } \mathbf{J}_i = \sigma_i \mathbf{E}_i. \tag{2}$$

where σ_i is the conductivity of each medium and V_i is the potential of a position. The total current I_{total} flowing through the system is calculated by integrating the current density across the interface areas of each medium:

$$I_{\text{total}} = \sum_{i} \iint_{S_i} \mathbf{J}_i \cdot d\mathbf{s_i},\tag{3}$$

where S_i is the surface region through which current flows between media. The value of S_i is dependent on the dimension of each medium.

Once the total current is determined, the system's overall conductance G_{total} and resistance R_g can be determined as follows:

$$G_{\text{total}} = \frac{I_{\text{total}}}{V_1}$$
 and $R_{\text{g}} = \frac{1}{G_{\text{total}}}$. (4)

The model shows how the intrinsic conductivities of a composite system's components influence the distribution of electric fields and currents when an external voltage is applied, ultimately determining the system's overall resistance. Secondly, after obtaining the numerical solution of R_g , the value of it is used for current and voltage mesh analysis [25] of the equivalent circuit model of the VFB system. This allows for the calculation of the voltage across R_g , thereby determining V_1 .

2.2.2. Potential difference composition analysis

The potential composition of the grounding system is illustrated in Fig. 5. It underscores the fact that the electric field and potential distribution under multiple boundary conditions cannot be accurately computed using simple calculations. This highlights the necessity of employing FEM analysis, which provides a more precise and effective numerical solutions based on boundary conditions in complex systems.

The potential difference between the leaked position and the zero potential ground can be divided into three parts.

(1) Potential difference between the leaked position and the electrolyte accumulated area Fig. 6 presents a zoomed view of the electrolyte leakage column and its accumulation area, illustrating their

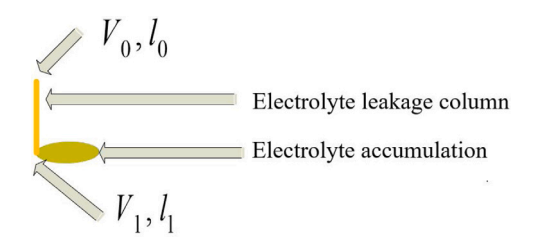


Fig. 6. Localised enlarged view of the leakage column and accumulation area.

positions and associated potentials. Since the leakage column is approximated as a cylindrical liquid column, the potential difference between its two ends can be calculated in the same manner as for a regular conductor (potential difference is the integral of the electric field). Therefore, the potential difference between the leaked position and the electrolyte accumulated area (top of the yellow column to the assumed circular area in Fig. 5 can be represented by the following formula:

$$V_0 - V_1 = \int_{l_0}^{l_1} \frac{J}{\sigma} \, dl \tag{5}$$

where J is current density, σ is conductivity of the medium, and l represents the length of the path along which the current is flowing. Then, the current that goes through the leaked electrolyte I_{le} can be calculated by:

$$I_{\rm le} = \frac{V_0 - V_1}{R_{\rm le}} \tag{6}$$

where R_{le} is the resistance of the leaked electrolyte.

(2) Potential difference between electrolyte accumulated circular area and the interface with soil ground

The potential difference between the electrolyte accumulated circular area and the interface with soil ground is presented in the blue cuboid concrete slab in Fig. 5. Assume that the accumulated electrified electrolyte region forms a specific circular area on the concrete medium's surface. The electromagnetic fundamentals dictate that the electric field direction within the applied potential area is perpendicular to the application medium's surface, pointing towards lower potential areas. Thus, around the voltage applied area, equipotential surfaces will form concentric circles centred on the application point. Since electric field lines are always perpendicular to equipotential surfaces, these surfaces will be parallel to the medium's surface and expand outward from the voltage application area. Although the electric field direction is always perpendicular to the surface of the medium, the propagation of the electric field is constrained by the dimensions of the medium. However, each medium possesses different dielectric constants and conductivities, resulting in non-uniform electric field distributions within each medium.

(3) Potential difference between the soil surface and the zero potential ground

The potential difference between the soil surface and the zero potential ground is shown in the red cuboid in Fig. 5. Although the electric potential begins to decay from the soil surface and eventually decays to a zero potential at the bottom of the soil ground, the propagation of the electric field within the soil ground is similar to its propagation within concrete. The electric field in the soil is also a non-uniform electric field, subject to the dimensions and material properties of the soil ground. Therefore, it cannot be obtained through simple calculations.

2.2.3. FEM analysis for potential and electric field distribution

Section 2.2.2 has demonstrated that simple calculations are inadequate for handling the potential and electric field distributions in multi-material systems with complex structures and boundary conditions. Moreover, in general electrical safety assessments, the grounding conductor is often modelled as a hemispherical contact surface in

direct contact with the ground, relying on simple calculations [26–28]. However, this approach is inadequate for assessing safety risks in multimaterial systems. It overlooks complex interactions between different media and excludes human body models, which are crucial for accurately evaluating the effects of electric fields and potential differences on human safety.

FEM is particularly effective for multi-material systems, as it accurately handles spatial variations in material properties, interfaces between different media, and complex boundary conditions, providing precise solutions for electric field and potential distributions.

Several first principles are needed for the FEM analysis. Gauss's law, as depicted within Maxwell's equations, elucidates that the net electric displacement flux emanating from a volume is equivalent to the charge contained within that volume. The differential form of Gauss's law for electricity is:

$$\nabla \cdot \mathbf{D} = \rho \tag{7}$$

where ${\bf D}$ is electric displacement or electric flux density, ∇ denotes the divergence of ${\bf D}$ and ρ is electric charge density. Since the electric charge density is related to the amount of charge per unit volume at a given spatial position, this variable is inherently dependent on the dimensions of each medium. In the context of multi-medium systems involving various materials, a detailed description of the electric flux density is necessary due to its dependence on the material properties. Constitutive relations delineate the relationship between the electric field and the electric flux density, often defined by the permittivity and conductivity of the materials involved. These relations are essential for characterising the behaviour of electromagnetic fields within heterogeneous mediums.

According to constitutive relations, the relationship between the electric displacement D, electric field E and polarisation P in a material can be expressed as:

$$\mathbf{D} = \varepsilon_0 \mathbf{E} + \mathbf{P} \tag{8}$$

where ε_0 is the permittivity of free space. The electric polarisation vector **P** here represents the effect of the material's dipoles in response to the electric field.

For linear, isotropic, and nondispersive materials, the above equation simplifies to:

$$\mathbf{D} = \varepsilon \mathbf{E} \tag{9}$$

where $\varepsilon = \varepsilon_0 \times \varepsilon_r$ is the dielectric constant of the material, and ε_r is the relative dielectric constant of the material.

Electric potential V at a point in space is a scalar quantity that represents the amount of work done per unit charge in bringing a positive test charge from infinity to that point. The gradient operator ∇ operates on a scalar field (in this case, the electric potential V resulted from the charged electrolyte) to produce a vector field (the electric field E). Geometrically, the gradient represents the direction and magnitude of the steepest ascent of a scalar field. The negative sign in $-\nabla V$ signifies that the electric field points in the direction of the greatest decrease in electric potential. This is because electric field lines always point from higher potential to lower potential, as objects naturally move from higher gravitational potential to lower gravitational potential. By combining these principles, the electric field can be articulated as:

$$\mathbf{E} = -\nabla V \tag{10}$$

combining Eq. (5), 7, and 8 yields Poisson's equation, which is used to express the electric potential V.

$$-\nabla \cdot (\varepsilon \nabla V) = \rho \tag{11}$$

The Poisson equation combined with potential boundary conditions, medium dimension boundary conditions, and material properties is used to quantify how charges distributed in space influence the electric

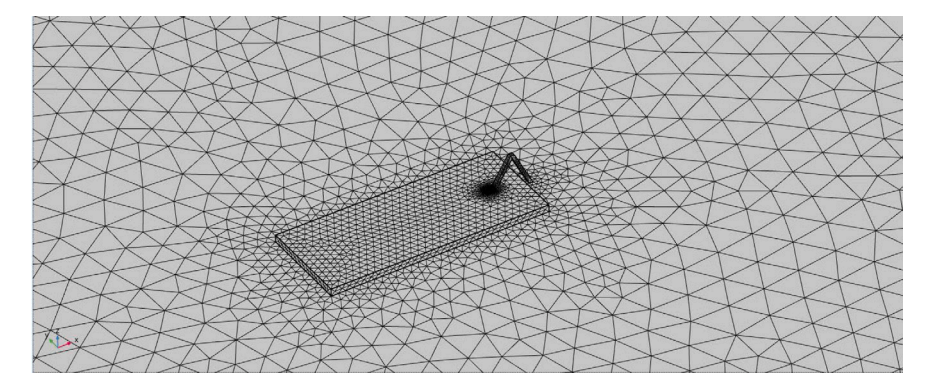


Fig. 7. Meshing of the grounding system for FEM analysis for Case 2-4.

potential throughout the region. Since the problem involves not only solving partial differential equations (PDEs) but also boundary conditions dependent on the dimensions of each medium (as referenced in Table 1), finite element method (FEM) analysis is required to accurately determine the electric field and potential distribution. Fig. 7 illustrates the meshing of the grounding system under the conditions described in Case 2-4.

The FEM accounts for media non-uniformity, such as spatial variations in dielectric constant and conductivity, thereby precisely calculating the non-uniform electric field's distribution across these media. By refining the mesh in regions where electric field strength significantly changes, FEM more accurately captures the details of the electric field and equipotential surfaces within non-uniform electric fields. Hence, when addressing the analytical challenges posed by non-uniform electric fields, especially when involving complex medium interfaces and notable spatial variations in electric field strength, the FEM offers a more precise numerical solution.

2.3. Equivalent body current analysis

Electrical safety assessment ultimately requires comparing the calculated equivalent body current with IEC standards to determine the associated electrical safety risks. Based on the results of the FEM analysis, the maximum and minimum potential (V_{max} and V_{min}) at the feet can be obtained. According to Ohm's Law, the current passing through the human body via foot-to-foot pathway can be expressed as:

$$I_{ff} = \frac{V_{pd}}{R_{ff}} \tag{12}$$

where $V_{pd}=V_{max}-V_{min}$ is the potential difference between two feet and R_{ff} is the resistance from foot to foot in the leg-crotch model and is part of the grounding system. According to IEC TS 60479, the equivalent current passing through the hand-to-feet path I_b can be obtained by multiplying a current-heart factor (F_{chf}) with I_{ff} [29]:

$$I_b = I_{ff} \times F_{chf}. \tag{13}$$

2.4. Electrical safety assessment procedure

The analysis steps of the proposed approach are as follows:

1. Grounding resistance analysis

Step 1: Initialise the analysis environment:

a. Set up potential boundary conditions: zero potential reference ($V_{ground}=0$) and user-defined terminal voltage $V_{terminal}$. (refer to Section 2.2.1)

b. Define analysis parameters: dimension of the concrete slab, soil ground and leg-crotch model, conductivity and dielectric constant. Note: $V_{terminal}$ is a user defined value to calculate the

Step 2: Meshing multi-medium grounding structures

a. Define material characteristics of each medium

equivalent ground resistance of the system.

- b. Construction and meshing of medium structures in Fig. 7
- Step 3: Conduct FEM analysis (refer to Section 2.2.1)
- Step 4: Obtain grounding resistance value

2. Leaked potential analysis

Step 1: Initialise the analysis environment:

- a. Define ionic resistance values for the electrolyte in all pathways of the VFB system (refer to Section 2.1.2)
- b. Incorporate R_g into the equivalent circuit model (refer to Section 2.2.1)
- c. Define electrical connection (Configuration 1 or 2) (refer to Section 2.1.1)
- Step 2: Use mass balance equations [18] and equivalent circuit model to conduct current and voltage mesh analysis (refer to Section 2.2.1)
- Step 3: Record maximum leaked position potential (V_0) and Potential across the grounding system (V_1) during VFB charging and discharging process
- 3. Potential and electric field distribution analysis

Step 1: Initialise the analysis environment:

- a. Set $V_{terminal} = V_1$ (V_1 is from leaked potential analysis)
- b. Check and keep media of material characteristics the same with grounding resistance analysis setting
- Step 2: Mesh the grounding system
- Step 3: Conduct FEM analysis for potential distribution and electric field distribution (refer to Section 2.2)
- Step 4: Collect maximum and minimum potential values within the feet area
- Step 5: Calculate the potential difference (refer to Section 2.3)
- 4. Leg-crotch model resistance analysis (refer to Section 2.3)

Step 1: Initialise the analysis environment:

- a. Define leg-crotch model material characteristics and model dimension
- b. Define a potential value added to the bottom of one foot

- c. Set zero potential reference
- Step 2: Conduct FEM analysis for resistance value of leg-crotch model R_{ff} (Ohm's law)
- Step 3: Collect leg-crotch model resistance value
- 5. Equivalent body current analysis and risk evaluation (refer to Section 2.3)
 - Step 1: Initialise the analysis environment:
 - a. Calculate the current via foot–foot pathway I_{ff}
 - b. Convert I_{ff} to equivalent body current via hand-to-feet pathway I_b
- Step 2: Determine the electrical safety risk using I_b based on DC current safety zone in Standard IEC 60479 [29], which is summarised in Appendix.

Note: A Simulink program and a COMSOL model were developed to conduct the simulation studies for the proposed electrical safety assessment in this paper. The Simulink model includes the electrical circuit model and the dynamic mass balance model of the VFB system. The COMSOL model is used for electric field simulations.

3. Case studies

The assumptions of the model used in the case studies are presented in Section 3.1 followed by the system parameters. Sections 3.2 to 3.5 present the simulation results of specific safety risks identified in the case studies. Section 3.6 offers a comparative analysis and discussion of the findings. In the simulation studies, the charging current and discharging current for the battery are set at 60 A and 48 A, respectively, undergoing continuous charge–discharge cycles. The mass balance equations employed in this study can be found in [18]. The VFB system is assumed to operate within the SOC range of 10% to 90%.

3.1. Model assumptions and system parameters

Based on the preceding analysis, the case studies will be conducted on the following assumptions. The mass balance equations for cells and assumptions related to these equations are same with [18]. Apart from the assumption in [18], the following assumptions are also considered:

- 1. The distance between the feet of the human body is maintained at 1 metre.
- 2. Continuous electrolyte leakage occurs.
- 3. Leaked electrolyte accumulates in an assumed circular area.
- 4. The electric potential decays to zero at a depth of 50 metres from the soil ground surface.
- 5. Continuous leakage occurs 0.2 m away from the bottom of the tank, maintaining constant contact with the contact surface.
- The resistance of the battery container is ignored as it is made of steel with small resistance

The system parameters are shown in Table 1.

3.2. Case 1: Low voltage configuration with two stacks in series (10 groups of it in parallel, 10P2S), without shoes protection

In Case 1, the electrical safety evaluation focuses on assessing the risks to the human body during the VFB electrolyte leakage operating under a low-voltage configuration. The evaluation examines three distinct grounding systems and considers the scenario in which individuals lack footwear protection. The potential and electric field distribution of Case 1 is shown in Fig. 8.

3.2.1. Case 1-1: Two feet on a large and wet concrete slab with leg-crotch model at edge of leakage accumulation without shoes protection-low voltage configuration

The electrical safety risks of continuous leakage in the VFB system operating in low-voltage mode (10P2S), when a large concrete slab is in a wet condition, with one foot at the edge of the leakage accumulation area and no footwear protection are evaluated in Case 1-1. In this scenario, a large concrete slab with the area of 20 m by 20 m (large) is positioned on the soil foundation. A VFB system is placed on the concrete and experiences a leakage at the tank, creating a circular contact area with a radius of 0.1 m on the concrete surface.

In assessing safety risks, only the most hazardous scenario is considered, with the maximum potential across from the leaked position to the ground (zero potential reference) when the SOC reaches its maximum. Following the procedure in Section 2.4, the equivalent grounding resistance R_g of this condition that combines multi-medium (a concrete slab, a soil ground model, and a leg crotch model) is found to be 1755.8 Ω . The dynamic leaked voltage during charging/discharging cycles is obtained by current and voltage mesh analysis of the VFB impedance network (the equivalent electrical circuit topology), as shown in Fig. 9), with a maximum leaked potential $V_{mlp} = 34.39$ V.

By applying the maximum leakage voltage to the electrolyte contact area and conducting FEM analysis, the electric field distribution can be attained. No shoe protections are taken into account in this case. As indicated in Fig. 8(a), the electrical potential is the highest at the area where the electrolyte accumulates, decreasing with increasing distance from the centre of the drop. Probes measure at the points of highest and lowest electrical potential (34.39 V and 18.47 V respectively) of feet areas. The potential difference between these two points is 15.92 V. Similar to R_g , R_{ff} can also be determined through resistance analysis, which is equal to 979.24 Ω (foot-to-foot path). This value remains unchanged when no additional footwear protection is applied to the human body model. Finally, by employing a heart current factor of 0.04 in Table A.4, the equivalent current I_b via hand-to-feet pathway can be calculated as follows:

$$I_{\rm b} = \frac{V_{\rm pd}}{R_{\rm ff}} \times F_{\rm chf} = 0.650 \text{ mA}$$
 (14)

The hazard level is determined as DC-1 in Table A.4, where the person involved may experience a slight pricking sensation.

3.2.2. Case 1-2: One foot on a small and wet concrete slab and the other foot on the soil with leg-crotch model at the edge of leakage accumulation and no shoes protection-low voltage configuration

In Case 1-2, the safety risks associated with continuous electrolyte leakage were assessed under a low voltage configuration (10P2S), in the presence of a small and wet concrete slab within the grounding system. The scenario involved a leg-crotch model with one foot placed on the concrete slab (at the edge of leakage accumulation) and the other on the soil ground, without the protection of footwear. This scenario specifies an area of concrete measuring 6 m by 2.5 m, which is much smaller compared to Case 1-1. Additionally, Case 1-2 posits that one foot is positioned on a wet concrete, while the other foot is placed on the soil ground with sandstone.

Due to the relocation of the components within the equivalent grounding system, value of $R_{\rm g}$ has changed. The analysis and calculations for Cases 1-2 yield $R_{\rm g}=1776.07\,\Omega$ and $V_{pd}=16.05\,{\rm V}$ and the resulting electric field distribution is shown in Fig. 8(b). The leg-crotch resistance R_{ff} is equal to 1036.18 Ω due to the extension in the shape. Hence, the equivalent current via the hand-to-foot pathway is determined to be $I_{\rm b}=0.620$ mA, which belongs to Zone DC-1.

Table 1
System parameters for electrical safety analysis.

V_{t}	3.445 m^3
V_{cell}	$1.28 \times 10^{-3} \text{ m}^3$
H_t	0.672 m
	20
	400
c	1.6 mol/L
S	1000 cm ²
d	$1.27 \times 10^{-4} \text{ m}$
E_a	17341 Jmol ⁻¹
R	$8.314 \text{ Jmol}^{-1} \text{ K}^{-1}$
R_c	$1 \Omega \text{ cm}^2$
R_d	$1.1 \Omega \text{ cm}^2$
	$4.66 \text{ m} \times 2.2 \text{ m} \times 2.42$
k_2	$4.88 \times 10^{-10} \text{ dm}^2 \text{ s}^{-1}$
k_3	$2.14 \times 10^{-10} \text{ dm}^2 \text{ s}^{-1}$
k_4	$7.33 \times 10^{-10} \text{ dm}^2 \text{ s}^{-1}$
k_5	$4.27 \times 10^{-10} \text{ dm}^2 \text{ s}^{-1}$
	279.76 m ⁻¹
	1128.38 m ⁻¹
	722.16 m ⁻¹
	$4.17 \times 10^4 \text{ m}^{-1}$
	261.15 m ⁻¹
	0.131 m^{-1}
	636.62 m ⁻¹
$\theta_{ m shoe}$	0.02 m
$S_{ m shoe}$	0.01 m ²
	6 m × 2.5 m × 0.2 n
	20 m × 20 m × 0.2 r
	50 m × 50 m × 50 n
	0.8 m
	$0.1 \text{ m} \times 0.1 \text{ m}$
	0.216 S/m
	80
	$1 \times 10^{-3} \text{ S/m}$
	3
	$1 \times 10^{-3} \text{ S/m}$
	10
	$1 \times 10^{-4} \text{ S/m}$
	6
σ_{ns}	6.67×10^{-3} S/m
	10
	2.0×10^{-8} S/m
r-	4
	V_{cell} H_t C S d E_a R R_c R_d k_2 k_3 k_4 k_5

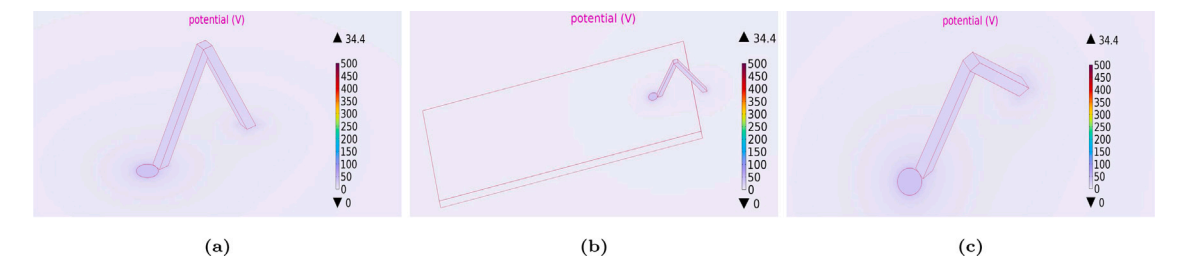


Fig. 8. Potential and electric field distribution of the VFB grounding system during leakage with human leg-crotch at the edge of leakage accumulation and no shoes protection in low voltage configuration (10P2S) (a) Case 1-1: Two feet on a large and wet concrete slab; (b) Case 1-2: One foot on a small and wet concrete slab and the other foot on the soil; (c) Case 1-3: Two feet on the soil ground, without concrete slab.

3.2.3. Case 1-3: Two feet on the soil ground with the leg-crotch model at the edge of leakage accumulation, without concrete slab and shoes protection-low voltage configuration

In Case 1-3, the evaluation focused on the electrical safety risks after the removal of the concrete slab from the grounding system, under a low voltage configuration (10P2S), with the leg-crotch model positioned at the edge of the leakage accumulation and without footwear protection. This case assessed the safety risks associated with a scenario where both the human body and the VFB are situated on the soil ground, and the VFB experiences a leakage.

In this scenario, there is no concrete slab, and the leg-crotch is placed directly on the soil ground. The analysis and calculations for Cases 1-3 lead to $R_g=1758.09\,\Omega$, $R_{ff}=979.24\,\Omega$ and $V_{pd}=16.04\,\mathrm{V}$ and the resulting electric field distribution is shown in Fig. 8(c). Hence, the equivalent current via the hand-to-foot pathway is determined to be $I_{\rm b}=0.655$ mA, which is within Zone DC-1.

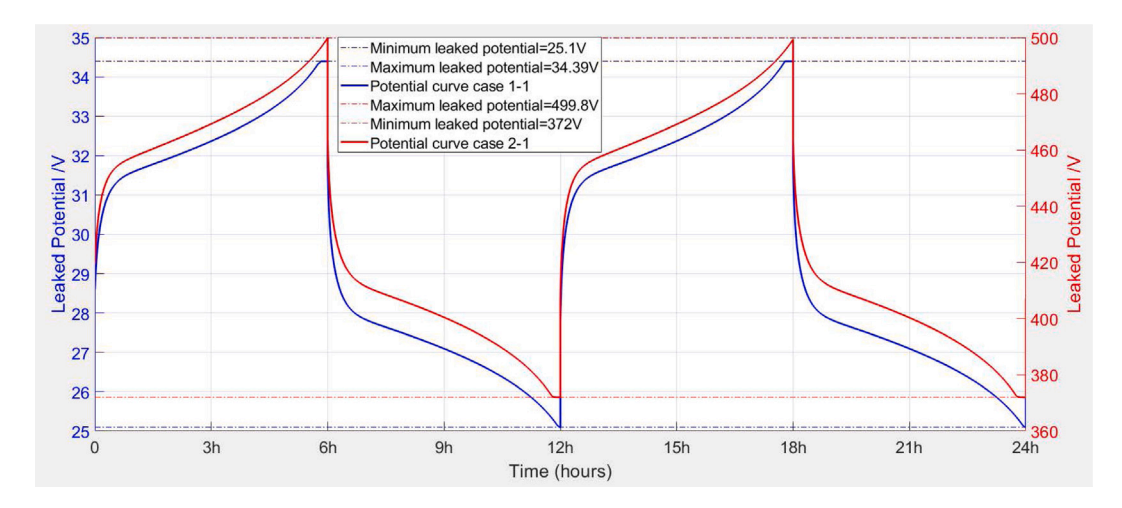


Fig. 9. Voltage across the equivalent grounding resistance under the same grounding system: (1) Case 1-1 (low voltage configuration, blue) (2) Case 2-1 (high voltage configuration, red)

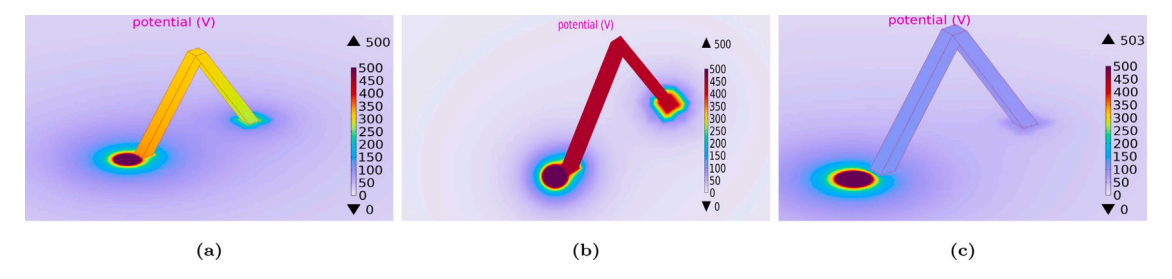


Fig. 10. Potential and electric field distribution of the VFB grounding system during leakage with two feet on a large concrete slab and no shoes protection in high voltage configuration (1P20S) (a) Case 2-1: Leg-crotch at the edge of leakage accumulation with a wet concrete; (b) Case 2-2: Other conditions same with (a) but with a dry concrete slab; (c) Case 2-3: Other conditions same with (a) but with leg-crotch 0.05 m away from leakage accumulation.

3.3. Case 2: High voltage configuration with 20 stacks in series (1P20S)

In Case 2, a hypothetical Configuration has been assumed where the 20 stacks are all connected in series to represent a high voltage system. This case evaluated the electrical safety risks under a high-voltage configuration in the three grounding systems considered in Case 1, without footwear protection, and investigated the safety margin. The investigation also explores the impact of the dryness level of part of internal media in the grounding system on electrical safety risks. The potential and electric field distribution of Case 2 is shown in Figs. 10 and 11.

The grounding system configuration in Case 2-1 to Case 2-3 remained consistent with that in Case 1-1. The configuration in Case 2-4 to Case 2-5 is the same as in Case 1-2. Similarly, the grounding configuration in Case 2-6 to Case 2-7 aligned with that in Case 1-3.

3.3.1. Case 2-1: Two feet on a large and wet concrete slab with leg-crotch model at edge of leakage accumulation and no shoes protection-high voltage configuration

Case 2-1 is an electrical safety assessment of continuous leakage in the VFB system, where all other conditions remain the same as in Case 1-1, except that the electrical configuration is changed to 20 stacks in series (1P20S).

The maximum terminal voltage is the sum of the voltages across the 20 stacks in this case. Both the R_g and R_{ff} stay constant (same with Case 1-1) because of the unchanged grounding model. The analysis and calculations for Cases 2-1 lead to $V_{pd}=231.44\,\mathrm{V}$ and the resulting electric field distribution is shown in Fig. 10(a). Therefore, the equivalent current via hand-to-feet pathway is derived to be $I_b=9.260\,\mathrm{mA}$, which belongs to Zone DC-2. This indicates that involuntary muscular contractions will occur with painful sensation.

3.3.2. Case 2-2: Two feet on a large and dry concrete slab with leg-crotch model at edge of leakage accumulation and no shoes protection-high voltage configuration

Case 2-2 assessed the electrical safety risks when R_g (from the area of applied leakage potential to the 0 potential reference) changes. Case 2-2 is based on Case 2-1, with a change in the moisture level of the concrete slab (conductivity of the concrete slab).

Keeping all other conditions of Case 2-1 constant, adjusting the moisture level of the concrete to dry condition and repeating same simulation procedures mentioned above, important analysis results can be attained, which are $R_g=11130.65\,\Omega$ and $V_{pd}=62.68\,\mathrm{V}$. The resulting electric field distribution is shown in Fig. 10(b). Hence, the equivalent body current via hand-to-feet is derived to be $I_\mathrm{b}=2.560\,\mathrm{mA}$., which belongs to Zone DC-1.

Compared to scenarios involving a wet concrete slab, the equivalent body current significantly decreases when a dry concrete slab is used. Therefore, with the same grounding system configuration, a grounding system with wetter concrete presents a higher electrical safety risk. According to IEC 60479-1, the perception threshold of DC current for the human body is 2 mA. However, due to variations in muscle distribution, physique, gender, and moisture levels, this perception threshold can fluctuate. To prevent the risk of falling due to electric shock sensation or muscle spasms, which could change the current path and lead to greater danger, such as a current exceeding 1 mA passing directly through the heart causing ventricular fibrillation (VF). Therefore, 1 mA is used as the safety current threshold, and the safety distance is determined based on this threshold.

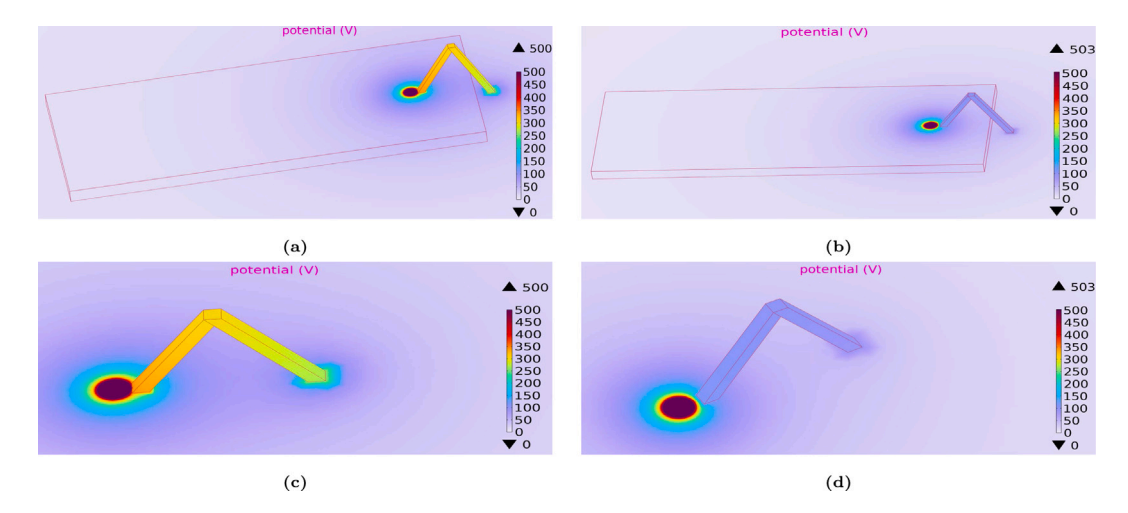


Fig. 11. Potential and electric field distribution of the VFB grounding system during leakage with no shoes protection in high voltage configuration (1P20S) (a) Case 2-4: One foot on a small and wet concrete slab and the other foot on the soil with leg-crotch at the edge of leakage accumulation; (b) Case 2-5: Other conditions same with (a) but with leg-crotch 0.05 m away from the leakage accumulation area; (c) Case 2-6: Two feet on the soil ground with leg-crotch model at the edge of leakage accumulation, without a concrete slab; (d) Case 2-7: Other conditions same with (c) but with leg-crotch 0.05 m away from the leakage accumulation area.

3.3.3. Case 2-3: Two feet on a large and wet concrete slab with leg-crotch model 0.05 $\,\mathrm{m}$ away from leakage accumulation and no shoes protection-high voltage configuration

Case 2-3 is an electrical safety assessment based on Case 2-1, with the leg-crotch model moved $0.05~\mathrm{m}$ away from the leakage accumulation area. The significance of Case 2-3 lies in providing a reference for defining a safety distance, as the equivalent human current in Case 2-1 indicated a safety risk.

The distance between the leg-crotch and edge of leakage accumulation is 0.05 m in Case 2-3. The increase in the distance between them leads to the change of R_g , which requires the reacquisition of the model's resistance. The analysis and calculations for Cases 2-3 result in $R_g=2376.48\,\Omega$ and $V_{pd}=20.98\,\mathrm{V}$ and Fig. 10(c) demonstrates the resulting electric field distribution. Thus, I_b can be determined to be $I_b=0.857\,\mathrm{mA}<1\,\mathrm{mA}$, indicating that the person will not fall due to current perception. Therefore, the greater dangers such as VF can be avoided and such a safety distance significantly reduces the risk.

3.3.4. Case 2-4: One foot on a small and wet concrete slab and the other foot on the soil with the leg-crotch model at the edge of leakage accumulation and no shoes protection-high voltage configuration

In Case 2-4, the electrical safety risks were evaluated based on the conditions in Case 1-2, with the only change being the replacement of the electrical configuration to a high voltage setup with 20 stacks in series (1P20S).

In this scenario, the electrical connection was modified to 20 stacks in series. The analysis results reveal that $R_g=1776.07~\Omega,~V_{pd}=233.23~\rm V.$ As illustrated in Fig. 11(a), the potential at the centre of the electric field aligns with the maximum voltage across the R_g . According to the analysis results, I_b is determined to be $I_b=9.000~\rm mA$, which is within Zone DC-2.

3.3.5. Case 2-5: One foot on a small and wet concrete slab and the other foot on the soil with the leg-crotch model 0.05 $\,\mathrm{m}$ away from leakage accumulation, and no shoes protection-high voltage configuration

In Case 2-5, the electrical safety assessment was conducted by maintaining all configurations from Case 2 while shifting the leg-crotch position 0.05 m away from the electrolyte leakage accumulation area. The electrical safety assessment results of Case 2-1 indicate a certain level of safety risk. The purpose of the electrical safety evaluation in Case 2-5 was to explore the risk level after establishing a specified safety distance.

Simulation results reveal that $R_g=2393.09\,\Omega$, $R_{ff}=1036.18\,\Omega$ and $V_{pd}=21.46$ V. The electric field distribution of the grounding system is

depicted in Fig. 11(b) and the equivalent current via the hand-to-foot pathway is determined to be $I_{\rm b}=0.828$ mA, which belongs to Zone DC-1.

3.3.6. Case 2-6: Two feet on the soil ground with the leg-crotch model at the edge of leakage accumulation, without concrete slab and shoes protection-high voltage configuration

In Case 2-6, the electrical safety risks were evaluated by modifying the electrical connection to a high voltage configuration with 20 stacks in series (1P20S), while keeping all other conditions from Case 1-3 unchanged. This scenario represents the most hazardous Configuration within Case 2.

In this scenario, $R_{\rm g}$ is same with Case 1-3. Simulation results reveal that $R_{\rm g}=1758.09\,\Omega$ and $V_{pd}=233.16\,{\rm V}$ and the potential and electric field distribution of the equivalent grounding model is illustrated in Fig. 11(c). Therefore, the equivalent current via the hand-to-foot pathway is determined to be $I_{\rm b}=9.520$ mA, which is within Zone DC-2.

Although 9.520 mA is significantly below the 50–75 mA (based on personal mass) threshold for DC let-go current and is unlikely to cause physiological effects, it is important to note that involuntary muscle contractions can occur within the DC-2 zone. Given that individuals have varying levels of tolerance to involuntary muscle spasms due to differences in physical constitution, it is necessary to take appropriate measures to reduce the equivalent percutaneous current.

3.3.7. Case 2-7: Two feet on the soil ground with the leg-crotch model 0.05 m away from the leakage accumulation, without concrete slab and shoes protection-high voltage configuration

In Case 2-7, an electrical safety risk assessment was conducted by moving the leg-crotch region 0.05 m further away from the leakage accumulation point, based on the setup in Case 2-6, to determine whether this safety distance is sufficient.

Case 2-6 demonstrates that I_b is approximately 10 mA, involuntary muscle twitching becomes inevitable. Consequently, it is essential to arrange a safety distance for the person. The analysis and calculations for Cases 2-7 result in $R_{\rm g}=2387.43\,\Omega$ and $V_{pd}=21.3\,{\rm V}$ and the resulting electric field distribution is shown in Fig. 11(d). Consequently, the equivalent current via the hand-to-foot pathway is determined to be $I_{\rm b}=0.870$ mA, which is within Zone DC-1.

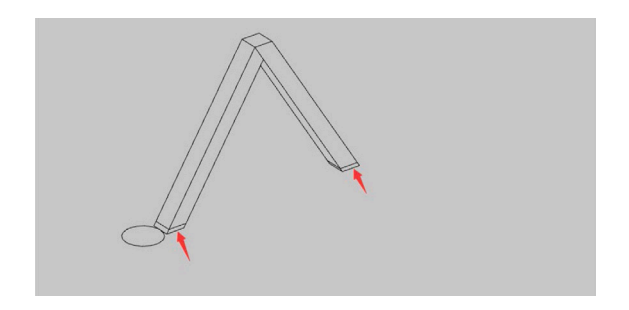


Fig. 12. Overview of leg components of a person with normal shoe material applied.

3.4. Case 3: Worst case of case 1 to case 2 without shoes

Comparing the equivalent body currents in scenarios without shoes from Cases 1 to Case 2, the maximum equivalent body current reaches approximately 10 mA. However, possible involuntary muscle contractions are also highly dangerous. This danger arises from the varying tolerance levels individuals have to such contractions, which can easily result in falls, subsequently altering the current path and increasing the overall risk.

3.5. Case 4: High voltage configuration with 20 stacks in series (1P20S), with shoes protection

Although the deployment regions for VFB systems may be proximal to infrastructure or leisure areas such as parks, it is not customary for all individuals to be barefoot in these zones. Hence, the electrical resistance offered by footwear should be considered when evaluating the risk of electric shock due to electrolyte leakage. Given the electrical resistance of non-protective ordinary footwear falls within the range of several hundred to several thousand ohms, and noting that this resistance value further decreases under wet conditions, this case study opts to select a lower feasible conductivity to simulate scenarios that pose a greater risk when wearing ordinary shoes.

The leg-crotch model in this case is modified from its original version by applying two pieces of sole material, each with a thickness θ_{shoe} (0.02 m), and an area S_{shoe} (0.1 m by 0.1 m), at the bottom of two feet, as illustrated in Fig. 12. FEM analysis results reflect potential and electric field distribution for all scenarios in case 4 as depicted in Fig. 13.

FEM analysis results reflect potential and electric field distribution for all scenarios in case 4 as depicted in Fig. 13. Given that Case 2-6 is the most hazardous among all the cases, Cases 4-1, 4-2, and 4-3 were conducted based on the analysis conditions of Case 2-6, with varying levels of footwear protection applied to the feet. The electrical safety risks were reassessed under these modified conditions to determine the impact of footwear protection on safety risk levels.

3.5.1. Case 4-1: Two feet on the soil ground without a concrete slab but with one foot at the edge of the electrolyte accumulation area and normal shoes protection-high voltage configuration (1P20S)

Case 4-1 assessed the electrical safety risks by adding standard footwear protection to the feet, based on the conditions in Case 2-6. This evaluation aimed to determine the impact of basic footwear protection on mitigating the electrical hazards present in the original case scenario.

In this scenario, normal shoes have been added to the bottom of the feet. Based on the conductivity and dielectric constant parameters of normal shoes in Table 1 and the dimensions of the footwear, the resistance of each shoe can be calculated as:

$$R = \rho \times \frac{l}{S} = 300.0 \ \Omega. \tag{15}$$

The analysis and calculations for this case yield $R_{\rm g}=2196.74\,\Omega$, and $V_{pd}=34.34\,\rm V$. The distribution of the potential and electric field can be attained as shown in Fig. 13(a). Thus, the equivalent body current via hand-to-feet pathway is determined to be $I_{\rm b}=1.400$ mA, which still exceeds 1 mA.

3.5.2. Case 4-2: Two feet on the soil ground without a concrete slab but with normal shoes protection and both feet 0.05 m back from the original position — high voltage configuration (1P20S)

Based on the analysis results of Case 4-1, it was observed that the body current could not be reduced below the safety threshold even with normal footwear protection. Therefore, in Case 4-2, the leg-crotch model is moved 0.05 m away from the leakage accumulation area to reassess the associated safety risks. The analysis and calculations $R_g = 2400.90\,\Omega$ and $V_{pd} = 16.48\,\mathrm{V}$ are derived. The potential and electric field distributions are determined through the FEM analysis, depicted in Fig. 13(b). Consequently, the equivalent current via the hand-to-foot pathway is determined to be $I_\mathrm{b} = 0.673\,\mathrm{mA}$, which belongs to Zone DC-1.

3.5.3. Case 4-3: Two feet on the soil ground without a concrete slab but with protection shoes and one foot at the edge of the electrolyte accumulation area — high voltage configuration (1P20S)

In case 4-3, an electrical safety assessment was conducted on the leg-crotch model after applying protective footwear to the feet.

Since batteries are commonly tested within their deployment areas, and there is a risk of electrolyte leakage during these tests, this case investigates whether wearing protective footwear mitigates the risk of step voltage electric shock in the event of electrolyte leakage. On the basis of case 4-1, the conductivity of the material is adjusted to σ_{ps} to ensure that the sole of the shoe provides a resistance protection of 100 M Ω with a lower dielectric constant as shown in Table 1.

The analysis and calculations for this case lead to $R_{\rm g}=2463.24~\Omega$ and $V_{pd}=0.0011~\rm V$. The potential and electric field distributions can be observed as shown in Fig. 13(c). Therefore, the equivalent passing through current via hand-to-feet pathway is determined to be $I_{\rm b}=4.50\times10^{-5}~\rm mA$, which is within Zone DC-1.

3.6. Results and discussion

In the scenario without shoes, the equivalent current passing through a person calculated in Case 2-6 is the highest, 9.520 mA. According to the classification of hazardous level for DC body current in Table A.3 in Appendix, the equivalent body current under the conditions of Case 2-6 falls within the DC-2 zone. Given that SOC of the VFB varies within a defined range during operation, the magnitude and direction of the current flow will change. This will inevitably lead to involuntary muscle contractions. Although the risk of VF is almost nonexistent, this scenario is not considered safe. This is due to the varying tolerance levels among individuals to involuntary muscle contractions. It cannot be guaranteed that such contractions will not lead to falls, potentially altering the path of the current through the body and posing greater risks, such as an equivalent current of over 1 mA passing directly through the heart, leading to ventricular fibrillation. According to IEC 60479-1, a slight pricking sensation will occur if direct current (DC) passing through the human body reaches approximately 2 mA. Additionally, body impedance significantly decreases when exposed to saltwater. Therefore, this paper adopts an equivalent through-body current of less than 1 mA as the standard for delineating safe areas.

Compared to the electrical connections under low voltage configuration, safety issues related to electrolyte leakage become more severe under high voltage configuration. This is due to the terminal voltage reaching its maximum as a result of all stacks being electrically connected in series.

Despite the fact that the value of R_g when concrete in a dry state exhibits a resistance value approximately sixfold higher than its wet

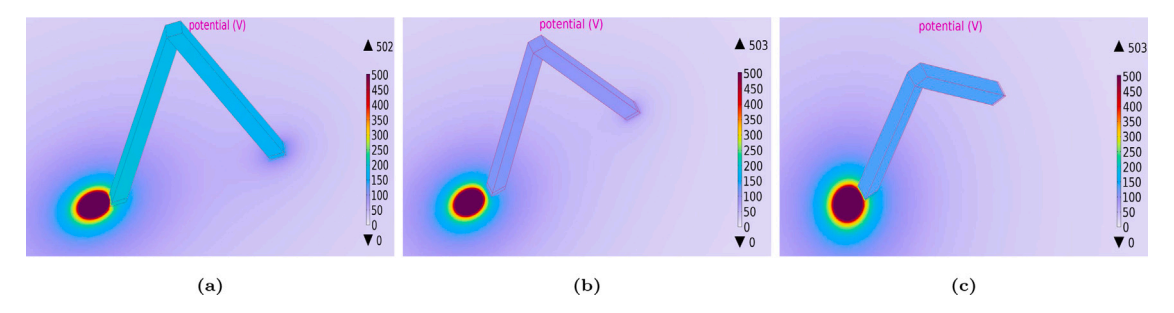


Fig. 13. Potential and electric field distribution of the VFB grounding system during leakage with shoes protection in high voltage configuration (1P20S) (a) Case 4-1: Two feet on the soil ground with leg-crotch model at the edge of leakage accumulation and normal footwear protection, without concrete slab; (b) Case 4-2: Other conditions same with (a) but with leg-crotch 0.05 m away from the leakage accumulation area; (c) Case 4-3: Other conditions same with (a) but with protective footwear protection.

counterpart, the constraints imposed by terminal voltage result in V_{mlp} in the case where dry concrete is applied marginally exceeding that observed under moist conditions. Simulation results indicate that when the concrete is dry, the current passing through a person under high voltage configuration is 2.560 mA, which is significantly lower than the 9.520 mA observed in wet conditions. This result can potentially be attributed to the increased resistance values when the concrete medium is dry. Under the condition where the human body resistance and applied voltage remain essentially unchanged, the increase in concrete resistance ultimately leads to a reduction in the current flowing through each component.

In an electric field, the electric potential decreases significantly as the distance from the centre of the field increases. Near the centre of the electric field, the potential changes rapidly, and the equipotential surfaces are closely spaced. Conversely, at locations farther from the centre of the electric field, the potential changes more gradually, leading to larger distances between equipotential surfaces. Therefore, when the foot closest to the centre of the electric field is at a distance of 0.05 metres from the area where the leaked electrolyte accumulates, the potential difference between the two feet is significantly reduced. This ultimately confines the current passing through the body to within a safe range.

In the most hazardous scenario displayed, Case 2-1 exhibits an equivalent human current slightly higher than Case 2-4, with values of 9.260 mA and 9.000 mA, respectively. However, it is not accurate to conclude that the risk of electric shock when both feet are on a concrete surface is higher than when one foot is on concrete and the other on a soil surface. This is because, in Case 2-4, with one foot on the soil and the other on concrete, the human body's resistance model is effectively elongated to make contact with the soil medium, resulting in a higher resistance compared to Case 2-1.

Considering the scenario where one foot is on the concrete surface and the other on the soil medium, maintaining the distance between the feet while ensuring that the leg resistance remains consistent with other cases presents challenges. This involves repeatedly altering the shape and using Ohm's law for multiple measurements to approximate the resistance values of the human leg-crotch found in other cases. Therefore, in Case 1-2, Case 2-4 and Case 2-5, an approach was adopted where one foot of the original leg-crotch model is partially elongated to enable contact with the soil medium.

In summary, Case 1 to Case 3 illustrate scenarios where the continuous leakage of electrolyte, under the condition of the feet being unshod, could pose a hazard. The simulation results indicate that for each case study, the maximum equivalent current passing through the leg-crotch ranges between 9 mA and 10 mA, all of which fall within the DC-2 zone, demonstrating the potential for significant risk under these conditions. In the case involving footwear, ordinary shoes with lower electrical resistance can offer a degree of protection, thereby reducing the equivalent current through a person to a certain extent. However, given the limited resistance protection that normal footwear provides, establishing a safe distance remains essential. Moreover, in

environments such as workspace, wearing protective footwear is highly recommended. This is because simulation results have shown that shoes with higher electrical resistance can offer substantial protection to the human body, reducing the equivalent current passing through a person to well below 1 mA, thus ensuring a higher level of safety.

Since the case studies discussed in this research are all plausible in real-world scenarios and the objective of this research is to assess safety risks under various conditions and to delineate safe zones, comparing which scenario is the most dangerous has little significance.

The above electrical safety analysis results are summarised in Table 2.

4. Conclusion

This paper presents an approach to analysing the electrical safety risks caused by electrolyte leakage of vanadium flow batteries. This study includes:

- Developing an equivalent circuit model during leakage containing all ionic resistance of electrolytes within its pathway of the VFB system and a leakage grounding path.
- Conducting FEM analysis on multi-medium grounding system to determine the grounding system resistance, potential and electric field distribution with the presence of the electrolyte leakage.
- Utilising the combination of the equivalent circuit model and the multi-medium grounding system to calculate the equivalent current pass the heart, which is used to evaluate electrical safety risk.

The case study results indicate that for a small commercial battery system with a capacity of 30 kW-130 kWh, the equivalent current through a person reaches its maximum when all stacks are electrically connected in series. Additionally, footwear can provide extra resistance protection to reduce this equivalent current. Establishing a safe distance is necessary, as when a person is positioned from the safety line to an infinitely distant point, the equivalent current through the body is insufficient to cause harm. In cases where footwear protection is unavailable, the risk of step potential electrocution due to continuous electrolyte leakage is the greatest, and the danger level can fall into the DC-2 zone when all stacks are electrically connected in series. Since this VFB system is typically used under low voltage configuration, and the simulation results indicate that the equivalent current through a person is less than 1 mA under this configuration, it is considered to pose no safety risk. However, according to IEC TS 60479, protective shoes should be regularly measured to ensure that their resistance has not significantly decreased due to ageing or other factors. Moreover, should the insulating material at the bottom of the footwear incur any damage, it must be replaced immediately. Additionally, the simulation results suggest that further increases in terminal voltage would lead to greater safety risks, especially when using larger battery systems. Once the equivalent current enters the DC-4 range, ventricular fibrillation becomes inevitable. Tolerance for a 10 mA current varies among

Table 2
Electrical safety analysis.

Cases	Dryness of concrete slab	Type of concrete slab	Type of shoes	Distance from leakage accumulation	Maximum leaked potential	Minimum leaked potential V_{mlp}	Current via hand-to-foot pathway							
								Case 1-1	Wet	Large	None	0 m	34.39 V	25.10 V
Case 1-2								Wet	Small	None	0 m	34.40 V	25.11 V	0.620 mA
Case 1-3	Wet	None	None	0 m	34.39 V	25.10 V	0.655 mA							
Case 2-1	Wet	Large	None	0 m	499.80 V	372.00 V	9.260 mA							
Case 2-2	Dry	Large	None	0 m	510.40 V	381.30 V	2.560 mA							
Case 2-3	Wet	Large	None	0.05 m	503.10 V	374.80 V	0.857 mA							
Case 2-4	Wet	Small	None	0 m	500.00 V	372.10 V	9.000 mA							
Case 2-5	Wet	Small	None	0.05 m	503.10 V	374.90 V	0.828 mA							
Case 2-6	Wet	None	None	0 m	499.90 V	372.00 V	9.520 mA							
Case 2-7	Wet	None	None	0.05 m	503.10 V	374.90 V	0.870 mA							
Case 4-1	Wet	None	Normal	0 m	502.30 V	374.20 V	1.400 mA							
Case 4-2	Wet	None	Normal	0.05 m	503.20 V	374.90 V	0.673 mA							
Case 4-3	Wet	None	Protective	0 m	503.40 V	375.10 V	$4.5 \times 10^{-5} \text{ m/s}$							

Note: Case 3 is the synthesis of the most hazardous scenarios from cases 1 and 2 without presenting new simulation results, it is not included in the table.

individuals and falls may happen as involuntary muscular contractions occur. While the body current under low voltage configuration remains safe, protective shoes are highly recommended under high voltage configurations. While the case studies are based on a specific commercial VFB system, the proposed approach can be applied to VFB systems with different configurations and power ratings, including those with higher system voltages which may lead to higher risks caused by electrolyte leakage.

CRediT authorship contribution statement

Bing Shu: Writing – review & editing, Writing – original draft, Visualization, Validation, Software, Methodology, Investigation, Formal analysis, Data curation, Conceptualization. Lai Wei: Writing – review & editing, Writing – original draft, Methodology, Investigation, Formal analysis, Conceptualization, Validation. Jie Bao: Writing – review & editing, Validation, Supervision, Resources, Project administration, Methodology, Funding acquisition, Conceptualization. Ke Meng: Supervision, Methodology, Conceptualization. Maria Skyllas-Kazacos: Writing – review & editing, Validation, Supervision, Methodology, Funding acquisition, Formal analysis, Conceptualization, Resources.

Declaration of competing interest

The authors declare the following financial interests/personal relationships which may be considered as potential competing interests: Jie Bao reports financial support was provided by Australian Research Council. Maria Skyllas-Kazacos reports financial support was provided by Australian Research Council. If there are other authors, they declare that they have no known competing financial interests or personal relationships that could have appeared to influence the work reported in this paper.

Acknowledgements

This work was supported by the Australian Research Council (ARC) Research Hub for Integrated Energy Storage Solutions (IH180100020) and North Harbour Clean Energy.

Appendix. IEC electrical safety standards

See Tables A.3 and A.4.

Data availability

Data will be made available on request.

Table A.3 Summary of current zones for hand-to-feet pathway (duration of current flow ≥ 2 s)

[29].		
Zones	Boundaries	Physiological effects
DC-1	Up to 2 mA	Slight pricking sensation possible when making, breaking, or rapidly altering current flow
DC-2	2 mA to 25 mA	Involuntary muscular contractions likely, especially when making, breaking, or rapidly altering current flow, but usually no harmful electrical physiological effects
DC-3	25 mA to 180 mA	Strong involuntary muscular reactions and reversible disturbances of formation and conduction of impulses in the heart may occur, increasing with current magnitude and time. Usually no organic damage to be expected
DC-4	>180 mA	Patho-physiological effects may occur such as cardiac arrest, breathing arrest, and burns or other cellular damage.

Note: For durations of current flow below 200 ms, ventricular fibrillation is only initiated within the vulnerable period if the relevant thresholds are surpassed. As regards ventricular fibrillation, this figure relates to the effects of current that flows in the path from left hand to feet and for upward current. For other current paths, the heart current factor has to be considered.

Table A.4
Heart-current factors for different current paths [29]

Heart-current factor F_{chf}
1.0
1.0
0.4
0.8
0.3
0.7
1.3
1.5
0.7
0.04

References

- E. Sum, M. Skyllas-Kazacos, A study of the V (II)/V (III) redox couple for redox flow cell applications, J. Power Sources 15 (2–3) (1985) 179–190.
- [2] E. Sum, M. Rychcik, M. Skyllas-Kazacos, Investigation of the V (V)/V (IV) system for use in the positive half-cell of a redox battery, J. Power Sources;(Switzerland) 16 (2) (1985).
- [3] M. Skyllas-Kazacos, M. Rychcik, R.G. Robins, A. Fane, M. Green, New all-vanadium redox flow cell, J. Electrochem. Soc. 133 (5) (1986) 1057.
- [4] M. Rychcik, M. Skyllas-Kazacos, Characteristics of a new all-vanadium redox flow battery, J. Power Sources 22 (1) (1988) 59–67.

- [5] A. Whitehead, T. Rabbow, M. Trampert, P. Pokorny, Critical safety features of the vanadium redox flow battery, J. Power Sources 351 (2017) 1–7.
- [6] C. Roth, J. Noack, M. Skyllas-Kazacos, Flow Batteries: From Fundamentals To Applications, John Wiley & Sons, 2022.
- [7] A. Trovò, G. Marini, W. Zamboni, S.D. Sessa, Redox flow batteries: A glance at safety and regulation issues, Electronics 12 (8) (2023) 1844.
- [8] N. Hagedorn, M.A. Hoberecht, L.H. Thaller, Nasa-Redox Cell-Stack Shunt Current, Pumping Power, and Cell-Performance Tradeoffs, Tech. rep., NASA Lewis Research Center, Cleveland, OH (United States), 1982.
- [9] P.R. Prokopius, Model for Calculating Electrolytic Shunt Path Losses in Large Electrochemical Energy Conversion Systems, NASA TM X-3359, 1976.
- [10] D.K. Slnaker, A. Lieberman, Nasa Technical Memorandum, NTIS Accession Number DE82000415.
- [11] E. Kaminski, R. Savinell, Technique for calculating shunt leakage and cell currents in bipolar stacks having divided or undivided cells, J. Electrochem. Soc., (United States) 130 (1983).
- [12] M.-Z. Yang, H. Wu, J.R. Selman, A model for bipolar current leakage in cell stacks with separate electrolyte loops, J. Appl. Electrochem. 19 (1989) 247–254.
- [13] R.E. White, C. Walton, H. Burney, R. Beaver, Predicting shunt currents in stacks of bipolar plate cells, J. Electrochem. Soc. 133 (3) (1986) 485.
- [14] H. Burney, R.E. White, Predicting shunt currents in stacks of bipolar plate cells with conducting manifolds, J. Electrochem. Soc. 135 (7) (1988) 1609.
- [15] K. Kanari, K. Nozaki, H. Kaneko, M. Kamimoto, Numerical analysis on shunt current in flow batteries, in: Proceedings of the 25th Intersociety Energy Conversion Engineering Conference, vol. 3, 1990, pp. 326–331, http://dx.doi. org/10.1109/IECEC.1990.716308.
- [16] G. Codina, J. Perez, M. Lopez-Atalaya, J. Vasquez, A. Aldaz, Development of a 0.1 kw power accumulation pilot plant based on an Fe/Cr redox flow battery part I. Considerations on flow-distribution design, J. Power Sources 48 (3) (1994) 293–302.
- [17] F. Xing, H. Zhang, X. Ma, Shunt current loss of the vanadium redox flow battery, J. Power Sources 196 (24) (2011) 10753–10757.

- [18] A. Tang, J. McCann, J. Bao, M. Skyllas-Kazacos, Investigation of the effect of shunt current on battery efficiency and stack temperature in vanadium redox flow battery, J. Power Sources 242 (2013) 349–356.
- [19] F. Wandschneider, S. Röhm, P. Fischer, K. Pinkwart, J. Tübke, H. Nirschl, A multi-stack simulation of shunt currents in vanadium redox flow batteries, J. Power Sources 261 (2014) 64–74.
- [20] Q. Ye, J. Hu, P. Cheng, Z. Ma, Design trade-offs among shunt current, pumping loss and compactness in the piping system of a multi-stack vanadium flow battery, J. Power Sources 296 (2015) 352–364.
- [21] X. Zhao, Y.-B. Kim, S. Jung, Shunt current analysis of vanadium redox flow battery system with multi-stack connections, J. Energy Storage 73 (2023) 100222
- [22] X. Guan, M. Skyllas-Kazacos, C. Menictas, An electrochemical stack model for aqueous organic flow battery: The mv/temptma system, Appl. Energy 375 (2024) 124024
- [23] M. Skyllas-Kazacos, M. Kazacos, State of charge monitoring methods for vanadium redox flow battery control, J. Power Sources 196 (20) (2011) 8822–8827.
- [24] D. Halliday, R. Resnick, J. Walker, Fundamentals of Physics, John Wiley & Sons, 2013.
- [25] M. Wang, Understandable Electric Circuits, The Institution of Engineering and Technology, 2010.
- [26] G. Parise, U. Grasselli, Simplified conservative measurements of touch and step voltages, in: IEEE Industrial and Commercial Power Systems Technical Conference, 1999, pp. 13–28.
- [27] M. Nayel, J. Zhao, J. He, Z. Cai, Q. Wang, Study of step and touch voltages in resistive/capacitive ground due to lightning stroke, in: 4th Asia-Pacific Conference on Environmental Electromagnetics, 2006, pp. 56–60.
- [28] A. Sunjerga, M. Rubinstein, D. Poljak, M. Despalatović, G. Petrović, F. Rachidi, High-frequency response of a hemispherical grounding electrode, Electr. Power Syst. Res. 226 (2024) 109877.
- [29] International Electrotechnical Commission (IEC), IEC TS 60479-1: Effects of Current on Human Beings and Livestock - Part 1: General Aspects, Technical Specification 60479-1, IEC, Geneva, Switzerland, 2023.